

Type 2 Immune Response Plays A Critical Role in Trained Immunity

Shih-Chin Cheng (✉ jamescheng@xmu.edu.cn)

Xiamen University <https://orcid.org/0000-0003-1251-8774>

Buyun Dang

Xiamen University

Jia Zhang

Xiamen University

Qingxiang Gao

Xiamen University

Qiumei Zhong

Xiamen University

Lishan Zhang

Xiamen University

Yanhui Zhu

Xiamen University

Junqiao Liu

Xiamen University

Yujia Niu

Xiamen University

Nengming Xiao

Xiamen University <https://orcid.org/0000-0001-5417-707X>

Wen-Hsien Liu

School of Life Sciences, Xiamen University <https://orcid.org/0000-0003-2500-3892>

Kairui Mao

xiaman University, China <https://orcid.org/0000-0003-2321-870X>

Shu-hai Lin

Xiamen University <https://orcid.org/0000-0002-4782-5320>

Jialiang Huang

Xiamen University

Stanley Huang

Case Western Reserve University <https://orcid.org/0000-0002-6557-3737>

Ping-Chih Ho

University of Lausanne <https://orcid.org/0000-0003-3078-3774>

Article

Keywords:

Posted Date: February 25th, 2022

DOI: <https://doi.org/10.21203/rs.3.rs-1322480/v1>

License:  This work is licensed under a Creative Commons Attribution 4.0 International License.

[Read Full License](#)

1 **Full Title: Type 2 immune response plays a critical role in trained immunity**

2
3 **Running Title: IL-4 induces trained immunity in macrophages**

4
5 **Authors**

6 Buyun Dang^{1#}, Jia Zhang^{1#}, Qingxiang Gao^{1#}, Qiumei Zhong¹, Li-shan Zhang¹, Yanhui Zhu¹, Junqiao Liu¹,
7 Yujia Niu¹, Nengming Xiao¹, Wen-Hsien Liu¹, Kairui Mao¹, Shuhai Lin¹, Jialiang Huang¹, Stanley Ching-
8 Cheng Huang³, Ping-Chih Ho^{4,5}, Shih-Chin Cheng^{1,2*}

9
10 **Affiliations**

11 ¹State Key Laboratory of Cellular Stress Biology, School of Life Sciences, Xiamen University,
12 Xiamen, Fujian, China.

13 ²Department of Gastroenterology, Zhongshan Hospital, School of Medicine, Xiamen University,
14 Xiamen, Fujian, China.

15 ³Department of Pathology, Case Western Reserve University School of Medicine, Cleveland, OH,
16 USA.

17 ⁴Ludwig Institute for Cancer Research, University of Lausanne, Epalinges, Vaud, Switzerland.

18 ⁵Department of Oncology, University of Lausanne, Epalinges, Switzerland.

19 #These authors contributed equally to this work.

20 *Corresponding author. Email: jamescheng@xmu.edu.cn

21 **Abstract**

22 Trained immunity, or innate immune memory, is vital in inducing heterologous protection against infection.
23 Type 2 cytokines such as IL-4 and IL-13 induce M2 macrophage differentiation, characterized by anti-
24 inflammatory phenotype permitting inflammation resolution and wound healing. Here we report that peritoneal
25 macrophages isolated from OVA-allergen sensitized mice possessed both M2 signatures and a pro-
26 inflammatory phenotype. Moreover, mice were more resistant to bacterial infection in the OVA-induced
27 allergy model. Mechanistically, we found that IL-4 induced trained immunity in a STAT6-independent and
28 IRS-dependent manner. Furthermore, IL-4 induces epigenetic memory in the pro-inflammatory gene enhancer
29 regions, ensuring a higher transcription activity upon stimulation. In addition, IL-4 trained macrophages are
30 metabolically more glycolytic upon LPS stimulation. To conclude, this unrecognized role of IL-4 in trained
31 immunity broadens our understanding of IL-4 mediated physiological changes and provides immediate impacts
32 on how type 2 immune response could re-direct disease progression in response to pathogen infection.

33 **Introduction**

34 Innate immunity as the sentinels of host immunity elicits rapid response towards intruding pathogens. Unlike
35 adaptive immunity, the self-nonsel self discrimination of innate immunity is antigen non-specific and acts via
36 germline-encoded pattern recognition receptors (PRRs). Therefore, immunological memory is regarded as an
37 exclusive characteristic of adaptive immunity that could form antigen-specific memory against the previously
38 encountered antigen. However, in the past decade, innate immune cells such as natural killer cells¹, monocytes²,
39 macrophages³ and neutrophils⁴ were reported to possess immunological memory in a limited-antigen specific
40 or antigen non-specific manner. This innate immunity memory is termed “trained immunity” , which is
41 mediated via metabolic rewiring and epigenetic reprogramming^{5,6}.

42 Based on the effector functions and pathophysiological effects, the innate and adaptive effector immunity could
43 be distinguished into type 1, type 2, and type 3 immunity, respectively⁷. Type 1 and 3 immunity are critical in
44 host defense against viral, bacterial and fungal infections. The dysregulated type 1 and 3 immunity also
45 regulates inflammatory and autoimmune diastases. Type 2 immunity is essential for protection against helminth
46 and venoms and is responsible for allergic and asthmatic diseases. IL-4 is one of the hallmark cytokines in
47 Type 2 immune response. The canonical role of IL-4 in inducing alternative activation in macrophages
48 (AAM ϕ), also known as M2^{8,9}, is extensively investigated. M2 macrophages are traditionally regarded as anti-
49 inflammatory macrophages, secreting Arginase-1, IL-10, TGF- β , and other anti-inflammatory cytokines,
50 promoting the resolution of inflammation and wound healing and favoring tumor development and progression
51 in the context of tumor-associated macrophages (TAMs). Upon binding to IL-4R α , IL-4 induces the
52 phosphorylation of STAT6, which in turn dimerizes and translocates into the nucleus for promoting
53 transcription of M2 signature genes.

54 Asthmatic patients had a decreased risk for hospital mortality, septicemia, sepsis, and septic shock across all
55 infections¹⁰. In a retrospective study, patients who survive *S. aureus* bacteremia have higher numbers of Th2
56 and fewer Th17 lymphocytes in the blood¹¹, suggesting that type 2 immune response might have a beneficial
57 bactericidal effect in humans. Furthermore, the accumulation of mast cells, eosinophils, and innate lymphoid
58 cells 2 (ILC2) have been suggested to engage in the bactericidal effect in the acute type 2 immune response¹¹.
59 Notably, trained immunity in macrophages has been demonstrated to be important in host anti-bacterial
60 response. We speculate that type 2 immunity might induce trained immunity in macrophages aiding in the anti-
61 bacterial effect. Here, we demonstrated that type 2 immune response primed macrophages to produce more
62 pro-inflammatory cytokines upon stimulation and rendered mice more resistant to bacterial infection. We
63 further uncovered a non-canonical feature of IL-4 in inducing "trained immunity". We delineated that different
64 sets of epigenetic reprogramming controlled the canonical M2- and non-canonical trained immunity-inducing
65 effects of IL-4. Therefore, we propose that IL-4 induces non-canonical trained immunity in macrophages via
66 epigenetic memory besides its well-characterized canonical anti-inflammatory role. This previously neglected

67 aspect of IL-4 biology might open up a new vista to broaden our understanding of the unresolved association
68 between asthma and other inflammatory diseases such as sepsis¹⁰ and obesity^{12,13}.

69 **Materials and Methods**

70 **Animals**

71 Wild-type C57BL/6 mice were purchased from Xiamen University Laboratory Animal Center. All mice were
72 maintained under specific pathogen-free conditions at the Xiamen University Laboratory Animal Center. These
73 mouse experiments were approved by the Institutional Animal Care and Use Committee. In addition, they were
74 in strict accordance with good animal practice as defined by the Xiamen University Laboratory Animal Center.

75 **Reagents**

76 Recombinant M-CSF (CB34), IL-4 (CK74), IL-5 (CW73), IL-13 (CX57), and IFN γ (CM41) were purchased
77 from Novoprotein, Shanghai, China. E. coli LPS (S11060), NT157 (S80314) were purchased from Shyuanye,
78 Shanghai, China. Syk inhibitor BAY 61-3606 (1615197-10-8) and Tunicamycin (11445) were purchased from
79 Cayman Chemical. BPTES, GSK-J4 (HY-15648B), Histone methyltransferase inhibitor MTA (HY-16938),
80 AS1517499 (HY-100614), and Etomoxir (HY-50202) were purchased from MedChemExpress. Wortmannin
81 (9545-26-7) was purchased from Adooq bioscience. GW5074 (R026615) was purchased from Rhawn,
82 Shanghai, China. SYBR Green Premix Pro Taq HS qPCR Kit (AG11701), Evo M-MLV reverse transcriptase
83 (AG11605), Recombinant RNase inhibitor (AG11608) were purchased from Accurate biology. Amplex Red
84 (119171-73-2) was purchased from Alfachem. N-(1-Naphthyl) ethylenediamine dihydrochloride (N9125) and
85 Sulfanilamide (S9251) were purchased from Sigma-Aldrich.

86 **Bone-Marrow-Derived Macrophage Culture and Differentiation**

87 Bone marrow cells were harvested from femurs and tibia of 6-8 week-old C56BL6/J mice and differentiated
88 in DMEM supplemented with 10 % FBS and 40 ng/ml of recombinant mouse M-CSF. Half volume of medium
89 containing fresh 40 ng/ml of M-CSF was added to the cell culture at day 3. Differentiated BMDMs were
90 detached, counted, and reseeded to the cell culture plate for subsequent experiments.

91 For macrophage polarization experiments, 20 ng/ml LPS and 100 ng/ml IFN γ were added to BMDMs to induce
92 M1 macrophage polarization. 20 ng/ml IL-4 were used to induce M2 polarization. To assess the short-term
93 effect of type II cytokines, BMDMs were cultured with 20 ng/ml of IL-4, IL-5, or IL-13. After 24 hours,
94 BMDMs were washed with PBS once and stimulated with 100 ng/ml LPS to assess the cytokine production
95 capacity. To assess IL-4 induced long-termed trained immunity, BMDMs were first cultured with 20 ng/ml IL-
96 4 for 24 hours and then washed with PBS once and refreshed with DMEM for additional 5 days. BMDMs were
97 then harvested for subsequent functional assessment. To assess the signaling pathways involved in IL-4
98 induced classic and non-classic effects, BMDMs were pre-incubated with various inhibitors for 30 min before
99 being stimulated with IL-4. BMDMs were washed with PBS 24 hours post-IL-4 stimulation and harvested for
100 subsequent functional assessment.

101 **Quantitative Real-Time PCR**

102 For quantitative RT-PCR, total mRNA was extracted with oligo-dT magnetic beads. In short, RNA was
103 extracted by magnetic beads conjugated with Oligo-dT18. Isolated RNA was reverse transcribed into cDNA
104 using dNTP (Beyotime, D7366) /oligodT mix, RNA transcriptase (Accurate Biology, AG11605), and RNase
105 inhibitor (Accurate Biology, AG11608). qPCR was performed using the SYBR Green method (Accurate
106 Biology, AG11701). Relative expression levels were calculated using the Δ CT method and normalized to the
107 expression of the β 2M housekeeping gene. The primer sequences we used are listed in Table S1.

108 **ELISA and Lactate Measurement**

109 Cytokine levels in culture supernatant or mice serum were determined by TNF- α (Invitrogen; 88-7324-88) and
110 IL-6 (Invitrogen; 88-7064-88) ELISA kits following the instructions of the manufacturer. As for lactate
111 measurements, the cellular supernatant was diluted by PBS. Then the diluent is mixed with the mixture
112 containing Amplex Red, HRP, and lactate oxidase for 10 min by one-to-one ratio. The fluorescence was
113 detected at excitation wavelength at 528 nm and emission wavelength at 590 nm.

114 **NO Measurement**

115 The cellular supernatant was mixed with solution A (ethylenediamine dihydrochloride) and solution B
116 (sulfanilamide) in a one-to-one ratio. Then the absorbance was measured at 540 nm.

117 **Western Blot**

118 Cells were lysed in RIPA buffer (1 mM Tris-HCl, 0.3 M NaCl, 0.01% SDS, 1.5% NP40, 120 mM deoxycholate,
119 1 M MgCl₂) containing protease inhibitors. Proteins were resolved by SDS-PAGE and transferred to PVDF
120 membranes (Roche, # 3010040001). The membranes were blocked for 1 h in blocking buffer (5% BSA and
121 0.1% Tween 20 in TBS) at room temperature and then incubated with respective primary antibodies in 5%
122 BSA at 4°C overnight. After being rinsed with TBST for three times, HRP coupled secondary antibodies in
123 TBST were used to blot for 1 h at room temperature. Antibody against β -Actin (21338) was purchased from
124 SAB. Antibodies against HK1 (A10886), HK3 (A8428), Glut1 (A11727), Histone H3(A2348), TriMethyl-
125 Histone H3K4 (A2357), Acetyl-Histone H3K27 (A7253) were purchased from ABclonal. Antibodies against
126 Mono-Methyl-Histone H3K4 (Clone D1A9, 5326S) were purchased from CST.

127 **Assay for Transposase-Accessible Chromatin with high-throughput sequencing (ATAC-seq)**

128 ATAC-seq was carried out mainly according to TruePrep DNA Library Prep Kit V2 for Illumina (Vazyme,
129 TD501) with minor modification. Briefly, we spun 30,000 cells at 500 g for 5 min. Cells were lysed for 10 min
130 at 4 °C by using pre-cold lysis buffer (10 mM Tris-HCl, pH 7.4, 10 mM NaCl, 3 mM MgCl₂ and 0.1% IGEPAL
131 CA-630). Nuclei were harvested for transposition reaction. After tagmentation, DNA was purified using the
132 Agencourt AMPure XP kit (Beckman Coulter, A63880). To reduce GC and size bias, we determined the final
133 PCR cycles using qPCR to allow library amplification to be stopped before saturation. We performed initial
134 amplifications for five cycles, after which we took an aliquot of the PCR reaction and added 10 μ l of the PCR

135 cocktail with SYBR Green at a final concentration of 0.3×. We ran this reaction for 25 cycles to calculate the
136 additional cycles required for the remaining 45 μL reaction. We amplified library fragments for 12-13 cycles.
137 The libraries performed double size selection for 300-500bp DNA fragments. Fragment distribution of libraries
138 was assessed with Agilent 4200. The library preparations were sequenced on an Illumina Hiseq platform, and
139 150 bp paired-end reads were generated.

140 **Cut&Tag-sequencing**

141 We adapted the Cleavage Under Target & Tagmentation (CUT&Tag) assay to perform chromatin-
142 immunoprecipitation sequencing. All procedures were carried out by following the manufacturer's instructions
143 described in NovoNGSR CUT&Tag 3.0 (Novoprotein, N259-YH01). Briefly, fresh cells were harvested and
144 counted. 10 μl concanavalin A-coated beads slurry were added to 100,000 cells to allow cell capture on an end-
145 over-end rotator for 10 min. Captured cells were separated by putting the tubes on a magnet stand. Primary
146 antibodies against H3K4me1 and H3K27ac were added to the cells at RT for 2 hr with gentle vortex. Secondary
147 antibody was added at RT for additional 1hr. Then mix pA/G-Tn5 adapter complex to a final concentration of
148 1:100 with 100 μL sample at RT for 1hr. After binding Tn5-adapter mixture, add 50 μL tagmentation buffer
149 at 37 °C for 1 hr. 10% SDS were added to stop tagmentation and solubilize DNA fragments at 55 °C for 10
150 min. Add 2 volume Tagment DNA Extract beads to the sample after termination. Beads were washed with
151 fresh 80% ethyl alcohol twice. Universal or barcoded i5/i7 primers were used for library amplification. Post-
152 PCR DNA library was purified with DNA Clean Beads followed by library quality inspection and Pair-end
153 Illumina sequencing.

154 **RNA Isolation and Sequence**

155 RNA from cells was isolated using RNAPrep Pure Cell/Bacteria Kit (TIANGEN) per instruction of the
156 manufacturer. RNA samples were quantified by Qubit and an Agilent Bioanalyzer for the RNA integrity
157 assessment. All samples had an RNA integrity number (RIN) of about 10. Following the manufacturer's
158 recommendations, sequencing libraries were generated using NEBNext® Ultra™ RNA Library Prep Kit for
159 Illumina® (NEB, USA), and index codes were added to attribute sequences to each sample. The clustering of
160 the index-coded samples was performed on a cBot Cluster Generation System using TruSeq PE Cluster Kit
161 v3-cBot-HS (Illumia) according to the manufacturer's instructions. After cluster generation, the library was
162 sequenced on an Illumina Novaseq platform, and 150 bp paired-end reads were generated.

163 **Metabolomics**

164 Bone marrow-derived macrophages (2×10^6) were seed in a 6-well plate and treated as above. Especially for
165 metabolites tracing experiment, DMEM was replaced with glucose-free medium supplemented with 12.5 mM
166 U-[¹³C]-glucose (Cambridge Isotope Laboratories) with or without 4 mM glutamine (Gibco). For metabolites
167 extraction, cells were washed three times with pre-cold PBS. After completely aspirating the liquid, the plates
168 were put on ice, 1 ml of extraction buffer (volume ratio 4:1 methanol/water) was added and scraped on ice.

169 The lysate was transferred to a 2 ml tube and vortex for 30 seconds, followed by additional 10 min sonication
170 in the ice bath, and then immediately frozen in a liquid nitrogen tank. The mixtures were centrifuged at 13,000
171 rpm for 15 min at 4 °C. Finally, supernatants were transferred to a new tube and lyophilized.

172 For metabolites analysis, the liquid chromatography with SCIEX Exion LC AD was prepared, and all
173 chromatographic separations were performed with a Millipore ZIC-pHILIC column (5 µm, 2.1× 100 mm
174 internal dimensions, PN: 1.50462.0001). Column was maintained at 40°C and the injection volume of all
175 samples was 2 µL. The mobile phase A composed by 15 mM ammonium acetate and 3 ml/L Ammonium
176 Hydroxide (> 28 %) in LC-MS grade water. The mobile phase B is composed by LC-MS grade 90 % (v/v)
177 acetonitrile in HPLC water. The mobile phase runs at a flow rate of 0.2 mL/min. The column was eluted with
178 the following gradient program: 95% B held for 2 min, increased to 45 % B in 13 min, held for 3 min, and the
179 post time was set 4 min. The QTRAP mass spectrometer used a Turbo V ion source. The ion source was run
180 in negative mode with a spray voltage of -4,500 V, Gas1 40 psi and Gas2 50 psi and Curtain gas 35 psi.
181 Metabolites were measured using the multiple reactions monitoring mode (MRM). The relative amounts of
182 metabolites were analyzed by MultiQuant Software Software (AB SCIEX).

183 **IL4c administration and LPS induced sepsis**

184 For the administration of IL-4 complex (IL-4c), 5 µg of recombinant mouse IL-4 was complexed to 25 µg of
185 anti-mouse IL-4 antibody (BioXCell,11B11), diluted in 200 µl of PBS and administered intraperitoneally. 24
186 hr post-IL-4c administration, mice were injected with 20 mg/kg LPS to induce sepsis. Serum was harvested
187 from the caudal tail 2 hr post-LPS injection. ELISA determined the IL-6 and TNF-α levels in serum according
188 to the manufacturer's instructions. Mice survival after LPS injection was monitored for 6 days.

189 **OVA-induced Allergy model**

190 C57BL/6 mice were intraperitoneally injected with 100 µg OVA (Sigma, A5253) absorbed to 10 % Alum
191 (Sigma, A6435) with the final volume ratio of OVA to Alum as 1:1 on days 0 and 14. Mice were
192 intraperitoneally injected with 0.1 mg OVA in 200 µl PBS from days 21 to 25. Mice were intraperitoneally
193 injected with *Staphylococcus aureus* at 5×10^3 CFU / 200 µL PBS per mouse. On day 26, whole blood from the
194 caudal tail was collected for calculating the CFU.

195 **RNA-seq data analysis**

196 Paired-end sequence reads were aligned to mouse genome reference (mm10) with HISAT2 and option as
197 defaults. These reads mapping to each gene were named raw-count through feature-count. FPKM of each gene
198 is based on the length of the gene and its raw count. The DESeq2 was used for differential gene expression
199 analysis. Differentially expressed genes were selected by fold change and significance relative based on two
200 biological replications. The significant genes show fold change above 2 with pvalues below 0.05.
201 ClusterProfiler (R) was used in pathway analysis and the resulting padj (pvalue adjusted using Benjamini and

202 Hochberg's) cut off 0.05. For clustering of M2 signature genes, the STEM program was used. RNAseq data
203 have been deposited in the GEO database with accession number GSE184811.

204 **GEO data analysis**

205 Data from GSE110465 were extracted by SRA-Toolkits. The reads were aligned to the mouse reference
206 genome (mm10) by bowtie2 program. Then, the peaks were called by MACS2 callpeak with option p-value
207 cutoff 0.01 and model fold 5-50.

208 All heatmap are created with ComplexHeatmap in R.

209 **Data Resource**

210 The accession number for the sequencing data reported in this paper is NCBI GEO: GSE184811(RNA-seq)
211 and GSE196099 (Cut&tag ATAC sequence).

212 **Statistics**

213 Differences were analyzed using the two-tailed Student's t-test. Analyses were performed using Prism
214 (GraphPad Software). Significant difference was label with star sign (p-value < 0.05). Data is shown as means
215 \pm SD.

216 **Results**

217 **Type 2 immune response induced trained immunity**

218 To examine whether type 2 immune response renders mice protection advantage against infection, we first
219 sensitized mice with OVA followed by *S. aureus* (SA) challenge (Fig. 1A). Mice experiencing acute OVA-
220 primed systemic allergy had delayed death upon lethal SA infection (Fig. 1B). The bacterial CFU in the blood
221 was significantly lower in the OVA-primed group, suggesting that acute allergy response induced enhanced
222 bactericidal effect (fig. S1A). Arg-1 and Rentla were explicitly upregulated in peritoneal macrophages isolated
223 from the OVA-primed group (Fig. 1C), confirming that acute allergic response triggered type 2 response and
224 induced M2 differentiation. Moreover, pro-inflammatory genes such as IL-6, IL-1 β , and NOS2 were
225 upregulated (Fig. 1D). Furthermore, OVA-primed mice were still more resistant to SA infection even 7 days
226 after the final OVA challenge (fig. S1B), suggesting acute allergy induced a long-lasting anti-bactericidal
227 effect. IL-5 induced eosinophilia has been shown to mediate bactericidal function in type 2 immune response¹¹.
228 Therefore, to exclude the confounding effect induced by IL-5 induced eosinophilia in OVA-allergy model, we
229 adopted another well-established IL-4c injection model to examine the role of macrophages¹⁴. To assess
230 whether IL-4c treatment also conditions M2 macrophages with higher pro-inflammatory potential, LPS were
231 injected into the peritoneal cavity one-day post-IL-4c injection. Serum (Fig. 1E) and peritoneal fluid (fig. S1C)
232 IL-6 and TNF- α levels were greatly enhanced upon LPS stimulation. In addition, IL-4c treated mice were more
233 susceptible to LPS sepsis (Fig. 1F), presumably due to the increased pro-inflammatory cytokine production.
234 Furthermore, IL-4c pre-treated mice were more resistant to SA infection (Fig. 1G), suggesting the acute IL-4
235 treatment protected mice from bacterial infection, similar to the protective effect observed in β -glucan induced

236 trained immunity¹⁵. In summary, these data suggest that type 2 immune response induces trained immunity,
237 such as producing more pro-inflammatory cytokines and more resistance to bacterial infection, in different
238 animal models.

239 **IL-4 induces trained immunity in macrophages**

240 Based on the animal data, we speculated that IL-4 might have dual function on macrophages. On the one hand,
241 IL-4 induced canonical M2 macrophages differentiation, while at the same time, IL-4 might train macrophages
242 to produce more pro-inflammatory cytokines upon stimulation. To test this hypothesis, we assessed whether
243 IL-4 could induce trained immunity in mouse bone marrow derived macrophages (BMDMs) as depicted in
244 Fig. 2A. As a result, IL-6, IL-12, and IL-1 β gene expression were upregulated (Fig. 2B), and the IL-6 protein
245 level and NO production were upregulated (Fig. 2C), suggesting the long-lasting effect of IL-4 treatment,
246 phenocopying the effect of the well-documented β -glucan induced trained immunity¹⁶. Noteworthy, the IL-
247 10 expression was downregulated (fig. S2A). In addition, BMDMs received activation signaling constitutively
248 from IL-4 for six days produced higher pro-inflammatory cytokines than the short-exposure group, suggesting
249 a prolonged type 2 stimulation could induce a heightened pro-inflammatory effect (fig. S2B).

250 We further performed RNAseq to acquire a panoramic view of the transcriptomic change of IL-4 induced
251 short-term (24 hours) and long-term (6 days) trained immunity. Gene expression profiles could be subdivided
252 into 9 clusters (Fig. 2D). Cluster 1-3 are enriched with genes downregulated by IL-4 at both time points. Cluster
253 6, 7, and 9 are genes upregulated at 24 hours post-IL-4 but declined or returned to basal at day 6. Cluster 5 and
254 8 are enriched with genes upregulated at day six but not significantly altered at 24 hours. Cluster 7 contains
255 M2 signature genes such as Arg1, Chil3, and Retnla, upregulated at 24 hours but returned to basal at day 6.
256 Gene Ontology enrichment analysis of different clusters suggests cytokine production biological process was
257 significant to downregulate in Cluster 1 and 3 (fig. S3A), and KEGG analysis suggesting that response against
258 multiple pathogens were also enriched in Cluster 3 (fig. S3B), reinforcing the role of IL-4 in the induction of
259 canonical anti-inflammatory response at basal state.

260 We further compared the gene expression profile upon LPS focusing on LPS upregulated genes. We subdivided
261 the differential expressed genes into 3 clusters: trained, unaffected and tolerant cluster by comparing the
262 expression level between control and IL-4 trained macrophages (Fig. 2E and fig. S4A). Pro-inflammatory
263 genes, such as IL-6, IL-12a, and IL-1b, were encompassed in the trained cluster at both 24 hours and day 6, in
264 line with the qPCR results (Fig. 2B). The GO enrichment analysis of the trained geneset also revealed the
265 enrichment of cytokine/chemokine activity (Fig. 2F), supporting the idea that the non-canonical feature of IL-
266 4 in promoting pro-inflammatory response.

267 Intrigued by the fact that IL-4 induces a more robust pro-inflammatory response in macrophages upon
268 stimulation, we wonder whether other type 2 cytokines could also induce trained immunity. We found out that
269 IL-13, but not IL-5, induced trained immunity in BMDMs as well (Fig. 2G & fig. S5), suggesting the signaling

270 transduction via IL-4R α is crucial in inducing trained immunity. Surprisingly, IFN γ failed to induce a long-
271 term pro-inflammatory phenotype, while stimulation with IFN γ and IL-4 simultaneously induced a similar
272 response as IL-4 single stimulation (fig. S5). These results imply that type 2 cytokine IL-4 and IL-13 induce
273 non-canonical trained immunity in BMDMs.

274 **IL-4 induces non-canonical pro-inflammatory feature in a Gln/ α -KG/jmjd3 axis- and STAT6- 275 independent but IRS-dependent manner**

276 Glutamine/ α -ketoglutarate/jmjd3 axis is critical for IL-4 induced M2 polarization^{17,18}. Therefore, to investigate
277 whether this axis is also responsible for the non-canonical feature of IL-4, BMDMs were stimulated with IL-4
278 in the presence or absence of glutamine. In line with the previous report, M2 signature genes such as Arg1 and
279 Chil3 were downregulated in glutamine-free conditions (Fig. 3A). In contrast, the pro-inflammatory gene (Fig.
280 3B&D) and protein expression (Fig. 3C&E) were not influenced both for short-term and long-term IL-4
281 stimulation. Similarly, inhibition with glutaminolysis or jmjd3 (Jumonji C domain containing 3) activity by
282 BPTES or GSK-J4, respectively, impaired M2 signature gene expression (fig. S6A&B), while upregulation of
283 IL-6 and downregulation of IL-10 were not altered (fig. S6C&D).

284 The STAT6 pathway is critical for IL-4 induced M2 polarization. We validated that STAT6 inhibition
285 downregulated M2 gene expression (Fig. S6E) and STAT6 phosphorylation (fig. S6F). However, pro-
286 inflammatory gene expression (Fig. 3F&G) and IL-6 protein and NO secretion (fig. S6G&H) were not
287 influenced by STAT6 inhibitor both at 24 hours or 6 days. These results suggest IL-4 induced non-canonical
288 trained immunity in a STAT6-independent manner.

289 Insulin receptor substrate (IRS) has been reported to transduce signals upon IL-4 stimulation¹⁹. Therefore, we
290 examine whether inhibition of IRS by NT-157 impacts IL-4 induced non-canonical effect. Pretreatment of
291 BMDMs with NT-157 significantly inhibited IL-4 induced pro-inflammatory gene expression (Fig. 3H).
292 Meanwhile, M2 gene expression was also impaired by NT-157 treatment (fig. S6I), suggesting the IRS signal
293 regulates IL-4 mediated canonical M2 differentiation and non-canonical pro-inflammatory feature.
294 Furthermore, western blot analysis indicates that NT-157 blocks IL-4 induced STAT6 phosphorylation (fig.
295 S6J), which partially explains why NT-157 inhibits M2 differentiation.

296 **IL-4 induces distinct epigenetic remodeling in M2 signature and trained gene sets**

297 Epigenetic modification and metabolic rewiring have been reported to be the two pillars underlying trained
298 immunity. Therefore, we first assessed IL-4 stimulation-induced epigenetic reprogramming by re-examining
299 the ATAC-seq data from the GEO database (GSE110465) to compare the chromatin accessibility of genes
300 regulated by IL-4 in BMDMs. As expected, M2 signature genes Arg1, Egr2, Retn1a, and Ccl24 had
301 constitutively accessible chromatin regions, and higher gene expression in IL-4 stimulated macrophages (fig.
302 S7A). In addition, the chromatin accessibility around the genes identified in the "trained" cluster, such as IL-6
303 and IL-12a, is also increased by IL-4 (fig. S7B). Noteworthy, IL-4 increases chromatin accessibility at distal

304 regulatory elements for genes in the trained cluster, while more relatively at promoter-proximal regions in the
305 M2 set (Fig. 4A).

306 H3K4me1 marked poised enhancer has been proposed to serve as a fingerprint of epigenetic memory regulating
307 the gene expression during embryonic cell development²⁰. We speculate that IL-4 induced trained immunity
308 might cause H3K4me1 marked poised enhancer around the "trained" genes, thus facilitating the higher
309 transcription activity upon subsequent stimulation. As H3K4me3 and H3K4me1 have previously been reported
310 to be the epigenetic landmark of β -glucan induced trained immunity in macrophages, we further examined the
311 epigenetic profiles of IL-4 trained macrophages by CUT & tag approach. The distal enhancers of
312 proinflammatory genes such as IL-6 and IL-12a were indeed marked with poised enhancer signatures with
313 enriched H3K4me1 peak but lack of ATAC and H3K27ac peaks (Fig 4B). Similar to the ATACseq result,
314 H3K4me1 peaks were more enriched at the distal region in the trained geneset (fig. S7C). The poised enhancer
315 bears epigenetic memory as the subsequent LPS stimulation resulted in higher proinflammatory gene
316 expression in IL-4 trained group (Fig 4C).

317 WDR5 forms a complex with MLL and Set H3K4 histone methyltransferase family. Knocking down of WDR5
318 partially inhibits IL-4 induced augmentation of IL-6 and IL-1 β expression (Fig. 4C & fig. S7D), suggesting a
319 potential role of H3K4 methylation in IL-4 induced trained immunity. These results imply that WDR5 mediated
320 H3K4me1 methylation might induce poised enhancers at the "trained" genes and results in the IL-4 induced
321 non-canonical trained immunity in macrophages. Furthermore, inhibition of histone methylation by MTA (pan-
322 methyltransferase inhibitor) impaired IL-4 induced IL-6 and IL-1 β gene expression (Fig. 4D) and the
323 production of IL-6 and NO (Fig. 4E), while MTA did not influence IL-4 induced M2 differentiation as
324 evidenced by the expression of Arg-1 and Rentla (fig. S7E). Putting together with the data from the glutamine
325 deficiency experiment, we speculate that IL-4, on the one hand, could induce canonical M2 gene expression
326 via Gln/ α -/jmd3/H3K27me3 axis^{17,18}. On the other hand, IL-4 induces non-canonical pro-inflammatory trained
327 immunity via H3K4me1 marked poised enhancer at the proinflammatory genes.

328 **IL-4 primed macrophages are more energetic and switch toward glycolysis upon LPS stimulation**

329 Upon stimulation, metabolic rewiring from oxidative phosphorylation to aerobic glycolysis is essential for
330 mounting efficient pro-inflammatory responses in macrophages. In addition, we previously reported that β -
331 glucan trained macrophages exhibit higher aerobic glycolysis metabolic status enabling a prompt response
332 upon stimulation²¹. We found that lactate production was significantly increased in IL-4 trained macrophages
333 upon LPS stimulation but not at the basal state (Fig. 5A). In line with the elevated lactate level, essential
334 glycolysis proteins such as HK3 and GLUT1 were also increased (Fig. 5B), indicating the elevated pro-
335 inflammatory feature of IL-4 trained macrophages possibly came from the robust shift towards glycolysis upon
336 LPS stimulation. However, 24 hours short-term IL-4 treatment does not upregulate HK3 and GLUT1 protein
337 levels, while IL-4 pre-treated macrophages still produce more lactate upon LPS stimulations (fig. S8A&B).

338 We further assess the effect of IL-4 on the energetic status both at acute (24 hours) or trained (6 days) states.
339 Acute IL-4 treatment increases macrophages' glycolysis and glycolytic capacity at basal and upon LPS
340 stimulation (Fig. 5C). Basal respiration, ATP production, and maximal respiration capacity are also increased
341 by acute IL-4 treatment (Fig. 5D). In line with the increased lactate secretion, IL-4 trained macrophages have
342 similar basal glycolysis compared to control macrophages. In contrast, trained macrophages upregulate
343 glycolysis upon LPS stimulation and have a higher glycolytic capacity (Fig. 5E). The OCR and mitochondrial
344 capacity of IL-4 trained macrophages had a similar pattern (Fig. 5F). Overall, IL-4 trained macrophages are
345 more energetic at the basal and upon stimulation (fig. S8C). We further performed stable isotope tracing in IL-
346 4 stimulated macrophages with the tracer [U-¹³C₆]-Glucose. In agreement with the Seahorse result (Fig. 5C),
347 ¹³C-labeled glycolytic intermediates were significantly increased in IL-4 stimulated macrophages (Fig. 5G).
348 The proportion of ¹³C-labeled TCA cycle intermediates, such as citrate, α-ketoglutarate, succinate, and
349 fumarate, was also primarily upregulated in IL-4 stimulated macrophages (fig. S8D), implying with higher
350 OXPHOS capacity and in line with the OCR result (Fig. 5D). Noteworthy, the elevated enrichment of ¹³C-
351 labeled α-ketoglutarate, succinate, and fumarate were blunted when macrophages were cultured in a glutamine-
352 free medium (fig. S8D). In agreement with the observed metabolic rewiring, the glycolysis, TCA cycle, and
353 glutamine metabolism genes were also upregulated in IL-4 stimulated macrophages (Fig. 5H). We further
354 performed metabolomics analysis for IL-4 stimulated BMDMs. Principle component analysis (PCA) suggests
355 that LPS stimulation induced a significant metabolic change at PC1, while LPS stimulated IL-4 day 6
356 macrophages further separated from the rest of the LPS stimulated group (fig. S9A). The TCA cycle and
357 glycolytic intermediates were increased in IL-4 trained macrophages at both time points (fig. S9B). Noticeably,
358 the one-carbon metabolism intermediates such as SAM and SAH are notably upregulated (Fig. S9C). The
359 elevated one-carbon metabolism might provide a methyl donor for IL-4 induced histone methylation.

360 **Discussion**

361 Type 2 immunity is critical for host defense against helminth infection and plays an essential role in allergic
362 and asthmatic diseases. IL-4 is one of the central cytokines upregulated in type 2 immune response. The
363 canonical function of IL-4 in inducing M2 macrophage differentiation and mediating anti-inflammatory
364 responses is well documented. The signaling transduction and pathway involved in IL-4 induced canonical
365 features are well characterized. However, an unrecognized non-canonical feature of IL-4 induction of trained
366 immunity has never been described. We report that type 2 immunity enhanced host bactericidal capacity via a
367 trained immunity mechanism. Pre-conditioning with IL-4 in acute type 2 immune response induced a non-
368 canonical, more robust responsiveness to microbial stimuli, similar to β-glucan-induced trained immunity,
369 upon stimulation in macrophages.

370 Metabolic rewiring and epigenetic control have been reported to play critical roles in the canonical M2
371 macrophage polarization. Jha et al. demonstrated that M2 polarization activates glutamine catabolism and

372 UDP-GlcNAc-associated modules²². When macrophages were polarized towards M2 in glutamine deprived
373 medium or with N-glycosylation inhibitor tunicamycin, M2 polarization and production of CCL22 were
374 significantly reduced. In addition, *jmjd3*, an H3K27me3 demethylase, has been reported to be upregulated by
375 IL-4 during M2 polarization, and knockdown of *jmjd3* also impairs M2 polarization *in vitro*²³. Furthermore,
376 helminth-induced M2 polarization is significantly reduced in *Jmjd3* *-/-* mice¹⁷. α -ketoglutarate has recently
377 been demonstrated to serve as a central hub bridging glutamine metabolism and *jmjd3*-mediated epigenetic
378 programming in M2 macrophages¹⁸. In addition to glutaminolysis, α -ketoglutarate is also derived as a by-
379 product of the de novo serine synthesis pathway via the upregulation of phosphoglycerate dehydrogenase
380 (*Phgdh*) activity induced by IL-4²⁴. Although the Gln/ α -KG/*jmjd3* axis has been demonstrated to be crucial for
381 IL-4 mediated M2 differentiation via downregulating H3K4me3, this axis is dispensable for the non-canonical
382 trained immunity induced by IL-4 in macrophages. Our data suggest that IL-4 treatment, on the one hand,
383 induces M2 gene expression via STAT6- and Gln/ α -KG/*jmjd3*-axis, which opens up the promoter region of
384 M2 signature genes by downregulation of the H3K27me3^{17,18}. On the other hand, IL-4 induces trained
385 immunity through an IRS-dependent manner and via recruiting WDR5 interacting H3K4 methyltransferase,
386 upregulating H3K4me1 around the enhancer region of the "trained" genes, including pro-inflammatory and
387 glycolysis genes. The H3K4me1 poised enhancer serves as epigenetic memory, facilitating a higher
388 transcription activity upon stimulation resulting in a more robust pro-inflammatory phenotype (Fig. 6).
389 The memory feature of innate immune memory or trained immunity differs from the antigen-specific memory
390 induced by adaptive immunity⁵. Instead, epigenetic reprogramming and metabolic rewiring are responsible for
391 the non-specific antigen augmentation of immune response responding to subsequent same or different
392 antigens in trained immunity²⁵. In the well-defined β -glucan trained immunity, enhanced glutaminolysis and
393 accumulation of fumarate induced by β -glucan stimulation are responsible for the H3K4me3 and H3K27ac in
394 the trained macrophages²⁶. In addition, β -glucan upregulated *Set7* methyltransferase and induced the
395 H3K4me1, thus increasing the *MDH2* and *SDHB* and oxidative phosphorylation capacity of trained
396 macrophages²⁷. Moreover, the rewired glycolysis capacity has been suggested to be critical for β -glucan
397 induced trained immunity both *in vitro* and *in vivo*¹⁶. The epigenetic memory could further be explained by the
398 existence of latent enhancers induced by external stimulation, which have a persistent effect mediating a faster
399 and more robust response upon stimulation²⁸. This latent enhancer-mediated epigenetic memory could be the
400 underlying mechanism of IL-4 induced non-canonical trained immunity, with the genes in the "trained" cluster
401 being robustly induced upon stimulation but remaining quiescent at the basal state.
402 Previous report suggested that type 2 immune response might render host a beneficial bactericidal effect (*10*,
403 *11*). Although the accumulation of eosinophils and ILC2 has been suggested to play a role in the bactericidal
404 effect in the acute type 2 immune response, here we uncovered the role of macrophages in the enhanced
405 bactericidal capacity. Acute IL-4c injection has been demonstrated to induce peritoneal macrophages

406 differentiation toward M2-biased phenotype²⁹. However, *ex vivo* stimulation of peritoneal macrophages with
407 IL-4 enhanced IL-6 and TNF- α production upon nematode *Neisseria meningitidis* infection³⁰ which is in
408 accordance with the non-canonical feature of IL-4 observed here. In addition to IL-4, another type 2 cytokine
409 IL-13, but not IL-5, could also induce trained immunity in macrophages *in vitro*. This prompts us to wonder
410 whether type 2 response could have an acute and chronic effect on macrophages *in vivo*. Mice injected with
411 IL-4c were more susceptible to LPS induced sepsis and secreted more IL-6 and TNF- α , suggesting acute IL-4
412 priming could enhance the pro-inflammatory response *in vivo*. This result is in line with a previous report
413 demonstrating that pretreatment with peritoneal macrophage with IL-4 augments the production of cytokines
414 and chemokines³¹. As trained immunity has been reported to possess a higher bactericidal effect in several
415 infection models¹⁶, we also found that IL-4 pretreatment mice were more resistant to an *S. aureus* infection. In
416 addition, type 2 immune response induced by OVA also renders mice better protection against the subsequent
417 bacterial infection. Moreover, the peritoneal macrophages from OVA-challenged mice have upregulated IL-6
418 production compared to control mice, suggesting that macrophages could acquire a pro-inflammatory
419 phenotype in the acute type 2 immune response. Therefore, our data suggest an acute type 2 immune response
420 could induce trained immunity *in vivo*. It would be worthwhile to examine whether circulating monocytes from
421 patient with acute allergic or post-allergic response bears trained immunity phenotype for the translational
422 purpose.

423 In contrast to our finding, Czimmerer et al. reported that IL-4 stimulated macrophages suppressed NLRP3
424 inflammasome activation and IL-1 β secretion upon LPS stimulation in a STAT6 dependent manner³². This
425 seemingly contradictory result could be due, at least partly, to the way of BMDMs differentiation. Czimmerer
426 et al. used a conditioned medium from L929 cells while we used recombinant M-CSF for BMDM
427 differentiation. As L929 conditioned medium contains M-CSF and other soluble factors, such as macrophage
428 migration inhibitory factor (MIF), osteopontin, Ccl2, and Ccl7, derived from L929, L929 conditioned medium
429 differentiated macrophages were functionally different from recombinant M-CSF derived macrophages³³. In
430 addition, Czimmerer et al. used *Helgmosomoides polygyrus* infection model to induce a type 2 immune
431 response in mice. However, instead of assessing the role of IL-4 on peritoneal macrophage by bacterial
432 infection, they examined the peritoneal macrophages isolated from *H. polygyrus* infected mice *ex vivo* and
433 showed that peritoneal macrophages from *H. polygyrus* infected group have lower Nlrp3 and Il1b expression
434 upon LPS stimulation. In contrast, we adopted a different model to assess whether a prior type 2 response could
435 induce the non-canonical effect of IL-4 *in vivo*, and the collective results point to the same effect that type 2
436 response causes a more robust pro-inflammatory response *in vivo* and renders a better protection capacity upon
437 bacterial infection.

438 Metabolically, IL-4 stimulated macrophages are more energetic with higher basal respiration rate and elevated
439 glycolysis at basal while switching toward robust glycolysis upon stimulation and have higher glycolytic

440 capacity. Metabolomics data reveal that IL-4 trained macrophages had elevated one-carbon metabolism, TCA
441 cycle, and glycolysis. The elevated one-carbon metabolism may provide SAM as a methyl donor for epigenetic
442 modification. Succinate accumulation might be responsible for the enhanced IL-1 β expression³⁴ and
443 subsequent H3K4me1 accumulation²⁷. Fumarate accumulation has been suggested to be involved in β -glucan
444 induced H3K4me3 accumulation²⁶. Therefore, the elevated intermediate TCA cycle metabolites accumulation
445 in IL-4 stimulated macrophages might impact IL-4 induced trained immunity via epigenetic modification.
446 To sum up, we propose that IL-4 induced both canonical M2 and non-canonical trained immunity via different
447 sets of epigenetic modifications. The non-canonical trained immunity induced by IL-4 is characterized by a
448 poised enhancer, enabling the trained macrophages to produce more pro-inflammatory cytokines upon
449 stimulation. Due to the association between asthma and chronic inflammatory diseases, such as obesity, or
450 asthma and acute inflammatory response, such as sepsis, we believe a further characterization of IL-4 induced
451 trained immunity will fill the gap of the Th2-biased disease asthma and chronic and acute inflammatory
452 diseases. Thus, our data here provide a new vista considering the well-characterized anti-inflammatory
453 cytokine IL-4 and offer a new horizon to cope with Th2 disease-associated inflammatory diseases.

454 455 **Acknowledgments**

456 S-CC was supported by National Natural Science Foundation of China (Grant number 32161133020 and
457 32070904) and Start-up fund of Xiamen University. P-CH was supported by European Research Council
458 Staring Grant 802773-MitoGuide, SNSF project grant 31003A_182470 and Cancer Research Institute. SC-CH
459 was supported by Cancer Research Institute CLIP Investigator Award, VeloSano and Comprehensive Cancer
460 Center American Cancer Society Pilot Grants IRG-91-022-19, IRG-16-186-21.

461 462 **Author contributions:**

463 Conceptualization: S-CC

464 Methodology: BD, JZ, QG, QZ, LZ, YH, JL

465 Investigation: BD, JZ, QG, SL, JH, SC-CH, P-CH, S-CC

466 Funding acquisition: S-CC

467 Supervision: S-CC

468 Writing – original draft: DB, JZ, S-CC

469 Writing – review & editing: DB, JZ, NX, W-SL, KM, SL, JH, SC-CH, P-CH, S-CC

470 **Conflict of interest**

471 Authors declare that they have no conflict of interest.

474 **References**

- 475 1 Sun JC, Beilke JN, Lanier LL. Adaptive immune features of natural killer cells. *Nature* 2009; **457**: 557–
476 561.
- 477 2 Kleinnijenhuis J, Quintin J, Preijers F, Joosten LAB, Ifrim DC, Saeed S *et al.* Bacille Calmette-Guerin
478 induces NOD2-dependent nonspecific protection from reinfection via epigenetic reprogramming of
479 monocytes. *Proc Natl Acad Sci U S A* 2012; **109**: 17537–17542.
- 480 3 Quintin J, Saeed S, Martens JHA, Giamarellos-Bourboulis EJ, Ifrim DC, Logie C *et al.* *Candida*
481 *albicans* infection affords protection against reinfection via functional reprogramming of monocytes.
482 *Cell Host and Microbe* 2012; **12**: 223–232.
- 483 4 Kalafati L, Kourtzelis I, Schulte-Schrepping J, Li X, Hatzioannou A, Grinenko T *et al.* Innate Immune
484 Training of Granulopoiesis Promotes Anti-tumor Activity. *Cell* 2020; **183**: 771–785.e12.
- 485 5 Netea MG, Joosten LAB, Latz E, Mills KHG, Natoli G, Stunnenberg HG *et al.* Trained immunity: A
486 program of innate immune memory in health and disease. *Science* 2016; **352**: aaf1098.
- 487 6 Netea MG, s JDXN-AX, Barreiro LB, Chavakis T, Divangahi M, Fuchs E *et al.* Defining trained
488 immunity and its role in health and disease. *Nature Reviews Immunology* 2020; : 1–14.
- 489 7 Annunziato F, Romagnani C, Romagnani S. The 3 major types of innate and adaptive cell-mediated
490 effector immunity. *J Allergy Clin Immunol* 2015; **135**: 626–635.
- 491 8 Orecchioni M, Ghosheh Y, Pramod AB, Ley K. Macrophage Polarization: Different Gene Signatures in
492 M1(LPS+) vs. Classically and M2(LPS-) vs. Alternatively Activated Macrophages. *Front Immunol*
493 2019; **10**: 1084.
- 494 9 Locati M, Curtale G, Mantovani A. Diversity, Mechanisms, and Significance of Macrophage Plasticity.
495 *Annu Rev Pathol* 2020; **15**: 123–147.
- 496 10 Zein JG, Love TE, Erzurum SC. Asthma Is Associated with a Lower Risk of Sepsis and Sepsis-related
497 Mortality. *Am J Respir Crit Care Med* 2017; **196**: 787–790.
- 498 11 Krishack PA, Louviere TJ, Decker TS, Kuzel TG, Greenberg JA, Camacho DF *et al.* Protection against
499 *Staphylococcus aureus* bacteremia-induced mortality depends on ILC2s and eosinophils. *JCI Insight*
500 2019; **4**. doi:10.1172/jci.insight.124168.
- 501 12 Peters U, Dixon AE, Forno E. Obesity and asthma. *Journal of Allergy and Clinical Immunology* 2018;
502 **141**: 1169–1179.
- 503 13 Bantulà M, Roca-Ferrer J, Arismendi E, Picado C. Asthma and Obesity: Two Diseases on the Rise and
504 Bridged by Inflammation. *J Clin Med* 2021; **10**: 169.
- 505 14 Huang SC-C, Smith AM, Everts B, Colonna M, Pearce EL, Schilling JD *et al.* Metabolic
506 Reprogramming Mediated by the mTORC2-IRF4 Signaling Axis Is Essential for Macrophage
507 Alternative Activation. *Immunity* 2016; **45**: 817–830.
- 508 15 Ciarlo E, Heinonen T, Théroude C, Asgari F, Le Roy D, Netea MG *et al.* Trained Immunity Confers
509 Broad-Spectrum Protection Against Bacterial Infections. *J Infect Dis* 2020; **222**: 1869–1881.

- 510 16 Cheng S-C, Quintin J, Cramer RA, Shepardson KM, Saeed S, Kumar V *et al.* mTOR- and HIF-1 α -
511 mediated aerobic glycolysis as metabolic basis for trained immunity. *Science* 2014; **345**: 1250684.
- 512 17 Satoh T, Takeuchi O, Vandenberg A, Yasuda K, Tanaka Y, Kumagai Y *et al.* The Jmjd3-Irf4 axis
513 regulates M2 macrophage polarization and host responses against helminth infection. *Nature*
514 *Immunology* 2010; **11**: 936–944.
- 515 18 Liu P-S, Wang H, Li X, Chao T, Teav T, Christen S *et al.* α -ketoglutarate orchestrates macrophage
516 activation through metabolic and epigenetic reprogramming. *Nature Immunology* 2017; **18**: 985–994.
- 517 19 Heller NM, Qi X, Junttila IS, Shirey KA, Vogel SN, Paul WE *et al.* Type I IL-4Rs selectively activate
518 IRS-2 to induce target gene expression in macrophages. *Sci Signal* 2008; **1**: ra17.
- 519 20 Bae S, Lesch BJ. H3K4me1 Distribution Predicts Transcription State and Poising at Promoters. *Front*
520 *Cell Dev Biol* 2020; **8**: 289.
- 521 21 Cheng S-C, Quintin J, Cramer RA, Shepardson KM, Saeed S, Kumar V *et al.* mTOR- and HIF-1 α -
522 mediated aerobic glycolysis as metabolic basis for trained immunity. *Science* 2014; **345**: 1250684.
- 523 22 Jha AK, Huang SC-C, Sergushichev A, Lampropoulou V, Ivanova Y, Loginicheva E *et al.* Network
524 integration of parallel metabolic and transcriptional data reveals metabolic modules that regulate
525 macrophage polarization. *Immunity* 2015; **42**: 419–430.
- 526 23 Ishii M, Wen H, Corsa CAS, Liu T, Coelho AL, Allen RM *et al.* Epigenetic regulation of the
527 alternatively activated macrophage phenotype. *Blood* 2009; **114**: 3244–3254.
- 528 24 Wilson JL, Nägele T, Linke M, Demel F, Fritsch SD, Mayr HK *et al.* Inverse Data-Driven Modeling
529 and Multiomics Analysis Reveals Phgdh as a Metabolic Checkpoint of Macrophage Polarization and
530 Proliferation. *CellReports* 2020; **30**: 1542–1552.e7.
- 531 25 Netea MG, Domínguez-Andrés J, Barreiro LB, Chavakis T, Divangahi M, Fuchs E *et al.* Defining
532 trained immunity and its role in health and disease. *Nature Reviews Immunology* 2020; **20**: 375–388.
- 533 26 Arts RJW, Novakovic B, Horst ter R, Carvalho A, Bekkering S, Lachmandas E *et al.* Glutaminolysis
534 and Fumarate Accumulation Integrate Immunometabolic and Epigenetic Programs in Trained Immunity.
535 *Cell Metabolism* 2016; **24**: 807–819.
- 536 27 Keating ST, Groh L, van der Heijden CDCC, Rodriguez H, Santos dos JC, Fanucchi S *et al.* The Set7
537 Lysine Methyltransferase Regulates Plasticity in Oxidative Phosphorylation Necessary for Trained
538 Immunity Induced by β -Glucan. *CellReports* 2020; **31**: 107548.
- 539 28 Ostuni R, Piccolo V, Barozzi I, Polletti S, Termanini A, Bonifacio S *et al.* Latent Enhancers Activated
540 by Stimulation in Differentiated Cells. *Cell* 2013; **152**: 157–171.
- 541 29 Jenkins SJ, Ruckerl D, Thomas GD, Hewitson JP, Duncan S, Brombacher F *et al.* IL-4 directly signals
542 tissue-resident macrophages to proliferate beyond homeostatic levels controlled by CSF-1. *J Exp Med*
543 2013; **210**: 2477–2491.
- 544 30 Varin A, Mukhopadhyay S, Herbein G, Gordon S. Alternative activation of macrophages by IL-4
545 impairs phagocytosis of pathogens but potentiates microbial-induced signalling and cytokine secretion.
546 *Blood* 2010; **115**: 353–362.

- 547 31 Major J, Fletcher JE, Hamilton TA. IL-4 pretreatment selectively enhances cytokine and chemokine
548 production in lipopolysaccharide-stimulated mouse peritoneal macrophages. *J Immunol* 2002; **168**:
549 2456–2463.
- 550 32 Czimmerer Z, Daniel B, Horvath A, Ruckerl D, Nagy G, Kiss M *et al.* The Transcription Factor STAT6
551 Mediates Direct Repression of Inflammatory Enhancers and Limits Activation of Alternatively
552 Polarized Macrophages. *Immunity* 2018; **48**: 75–90.e6.
- 553 33 Heap RE, Marín-Rubio JL, Peltier J, Heunis T, Dannoura A, Moore A *et al.* Proteomics characterisation
554 of the L929 cell supernatant and its role in BMDM differentiation. *Life Sci Alliance* 2021; **4**.
555 doi:10.26508/lisa.202000957.
- 556 34 Tannahill GM, Curtis AM, Adamik J, Palsson-McDermott EM, McGettrick AF, Goel G *et al.* Succinate
557 is an inflammatory signal that induces IL-1 β through HIF-1 α . *Nature* 2013; **496**: 238–242.

558 **Figures Legends**

559 **Figure 1. Type II immune response induced trained immunity *in vivo*.** (A) Schematic
560 presentation of mice OVA-allergy model. (B) Survival curve of control or OVA-primed mice after
561 *S. aureus* infection. (C) qPCR analysis of the M2 marker genes from peritoneal macrophages
562 isolated at day 25 from the OVA challenged or PBS control group. (D) Peritoneal macrophages
563 from the OVA challenged or PBS control group were stimulated with LPS for 4 hours *ex vivo*. The
564 expression of cytokine genes was determined by qPCR. *P < 0.05, unpaired, two-tailed Student's
565 t-test. Data are representative of 2 independent experiments with 10 mice per group (mean ± SD).
566 (E) IL-6 and TNF-α were determined from serum taken 3 hours post LPS injection in control and
567 IL-4c treated mice. Survival of wild-type C57BL/6J pre-treated with PBS or IL-4c for 24 hours
568 followed by (F) LPS i.p. injection or (G) *S. aureus* infection. Data are representative of 2
569 independent experiments with 10 mice per group.

571
572 **Figure 2. IL-4 induced non-canonical trained immunity in macrophages.** (A) Schematic
573 presentation of the experimental setup for assessing short-term or long-term IL-4 non-canonical
574 effect in macrophages. (B) Short-term (Day 2) or long-term (Day 6) IL-4 stimulated BMDMs were
575 stimulated with LPS for 4 hours, and mRNA was harvested for subsequent qPCR analysis. (C) IL-
576 6 and NO production were determined from the culture supernatant 24 hours post LPS stimulation.
577 (D) Differential gene expression analysis between the control, IL-4 24 hours stimulated, and IL-4
578 trained BMDMs at day 6 was presented as a heatmap. (E) Control and IL-4 24 hours stimulated
579 BMDMs were stimulated with LPS or left untreated for 4 hours. LPS upregulated genes were
580 filtered out, and the expression level was ranked normalized according to the Log2FC value
581 between the control-LPS group and IL-4-LPS group. Genes were further divided into three clusters:
582 trained ($\text{Log}_2\text{FC} \geq 0.5$), unaffected ($0.5 \geq \text{Log}_2\text{FC} \geq -0.5$), and tolerant ($\text{Log}_2\text{FC} \leq -0.5$). (F) Gene
583 ontology analysis of genes in the trained clusters. (G) IL-13 stimulated BMDMs were stimulated
584 with LPS for 4 hours, and mRNA was harvested for subsequent qPCR analysis for the expression
585 of IL-6 and IL-12. IL-6 and NO production were determined from the culture supernatant 24 hours
586 post LPS stimulation. *P < 0.05, unpaired, two-tailed Student's t-test. Data are representative of 3
587 independent experiments with 3 to 4 samples per group (mean ± SD).

588
589 **Figure 3. IL-4 induced trained immunity in a Gln/α-KG/jmjd3 axis-, STAT6-independent and**
590 **IRS-dependent manner.** qPCR mRNA expression of M2 marker genes (A), cytokine genes (B, D,
591 F, G&H) in BMDMs stimulated with IL-4 (A), or LPS (B, D, F, G&H) at 24 hours or day 6 post-

592 IL-4 stimulation under various culture condition as indicated. Corresponding IL-6 and NO
593 production were measured from supernatant harvested 24 hours post LPS stimulation (C&E). *P <
594 0.05, unpaired, two-tailed Student's t-test. Data are representative of 3 independent experiments
595 with 3 to 4 samples per group (mean ± SD).

596

597 **Fig. 4. Epigenetic modification shapes IL-4 induced trained immunity in macrophages.** (A)

598 Peak distributions of differential ATAC peaks in M2 upregulated gene set and trained gene set
599 between control and IL-4 treated BMDMs. (B) Representative ATACseq H3K4me1, H3K4ac CUT
600 & tag screenshots of control or IL-4 24h and day 6 stimulated BMDMs in the gene region pro-
601 inflammatory genes IL-6 and IL-12a. The dashed box pointed to the poised enhancer region. (C)
602 The gene expression profile of selected genes at basal state or 4h-post LPS stimulation. (D) Control
603 or WDR5 stable knockdown Raw264.7 cells were pre-treated with IL-4 for 24 hours and stimulated
604 with LPS for 4 hours to assess the mRNA expression of IL-6 and IL-1β by qPCR. (E) qPCR mRNA
605 expression of cytokine genes in BMDMs pre-treated with MTA for 30 minutes followed by 24
606 hours IL-4 stimulation. The gene expression was determined 4 hours post LPS stimulation. (F) IL-
607 6 and NO production was determined from 24 hours supernatant post LPS stimulation. *P < 0.05,
608 unpaired, two-tailed Student's t-test. Data are representative of 3 independent experiments with 3
609 samples per group (mean ± SD).

610

611 **Figure 5. Metabolic characterization of IL-4 induced trained immunity in macrophages.** (A)

612 IL-4 trained BMDMs at day 6 were stimulated with LPS. The supernatant was harvested 24 hours
613 post LPS, and lactate level was determined. (B) Western blot from cell lysate harvested from control
614 or IL-4 trained BMDMs at day 6 or 3 hours post LPS stimulation. Antibodies specific for
615 endogenous GLUT1, HK3 and actin were used to blot the target protein. Representative blots of
616 three independent experiments are shown. Seahorse analysis of control or IL-4 induced trained
617 BMDMs at both acute (24h) or trained (6 days) at basal or 3 hours post LPS stimulation. ECAR
618 and glycolysis capacity (C&E) and OCR and mitochondrial respiration capacity (D&F) were
619 determined from two independent experiments. (G) Representative metabolites derived from ¹³C₆-
620 Glucose following the glycolysis pathway determined by LC-MS were shown. (H) Differential
621 gene expression in glycolysis, TCA cycle, and glutamine metabolism between the control, IL-4 24
622 hours stimulated, and IL-4 trained BMDMs at day 6 was presented as a heatmap.

623

624 **Fig. 6. Schematic model of IL-4 induced canonical and non-canonical responses.**

Figures

Figure 1

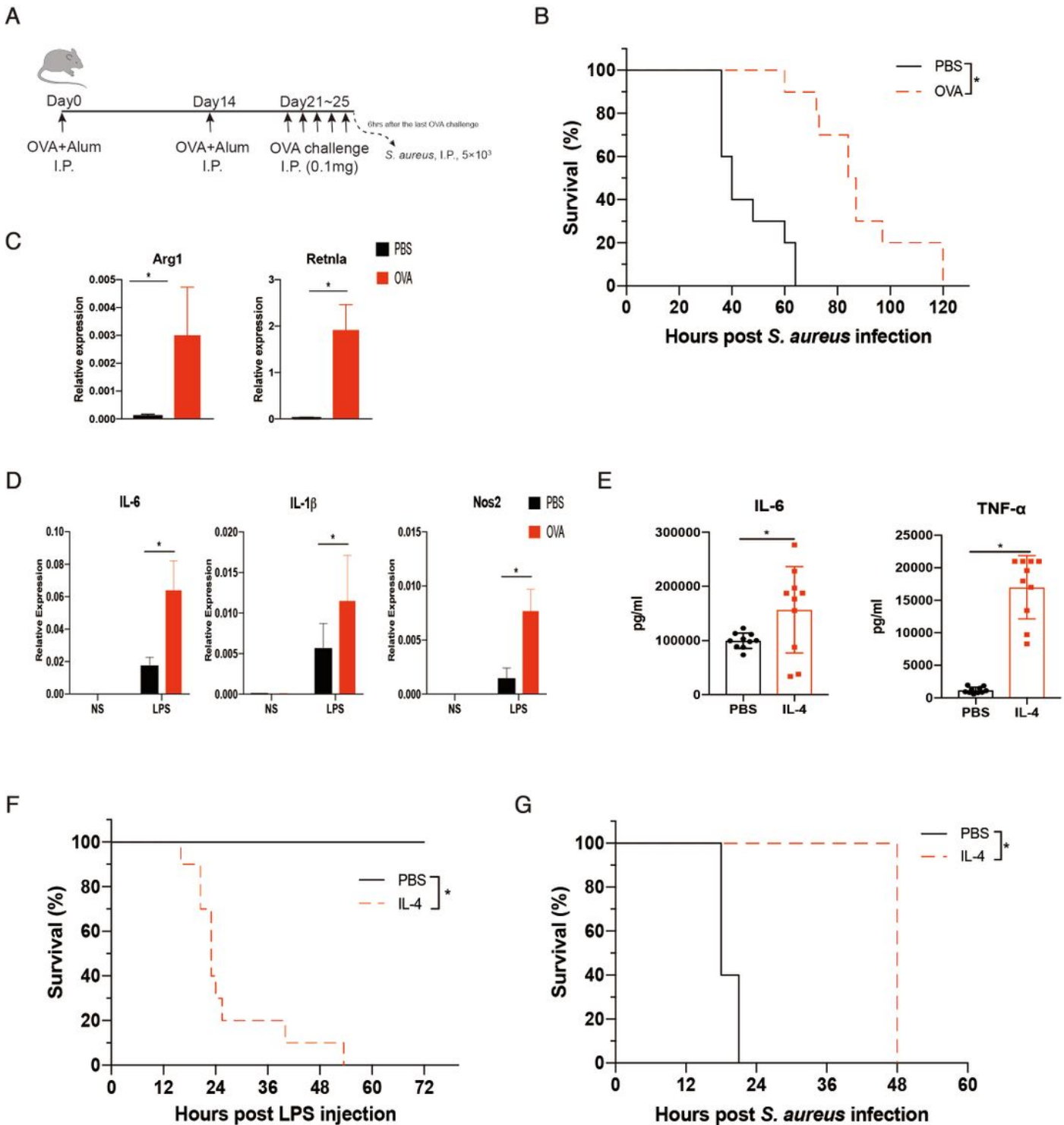


Figure 1

Type II immune response induced trained immunity *in vivo*. (A) Schematic presentation of mice OVA-allergy model. (B) Survival curve of control or OVA-primed mice after *S. aureus* infection. (C) qPCR analysis of the M2 marker genes from peritoneal macrophages isolated at day 25 from the OVA

challenged or PBS control group. (D) Peritoneal macrophages from the OVA challenged or PBS control group were stimulated with LPS for 4 hours *ex vivo*. The expression of cytokine genes was determined by qPCR. *P < 0.05, unpaired, two-tailed Student's t-test. Data are representative of 2 independent experiments with 10 mice per group (mean ± SD). (E) IL-6 and TNF-α were determined from serum taken 3 hours post LPS injection in control and IL-4c treated mice. Survival of wild-type C57BL/6J pre-treated with PBS or IL-4c for 24 hours followed by (F) LPS i.p. injection or (G) *S. aureus* infection. Data are representative of 2 independent experiments with 10 mice per group.

Figure 2

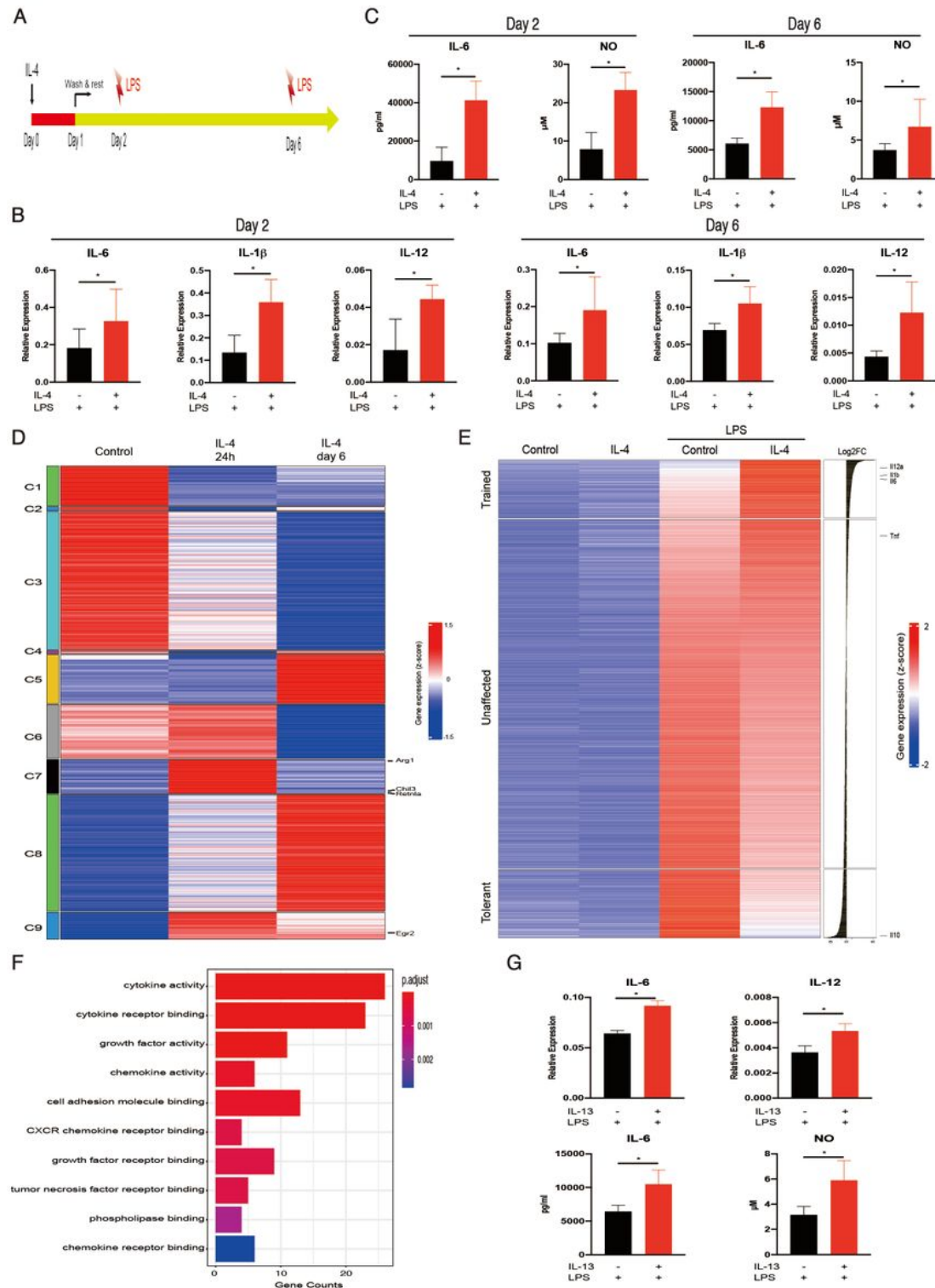


Figure 2

IL-4 induced non-canonical trained immunity in macrophages. (A) Schematic presentation of the experimental setup for assessing short-term or long-term IL-4 non-canonical effect in macrophages. (B) Short-term (Day 2) or long-term (Day 6) IL-4 stimulated BMDMs were stimulated with LPS for 4 hours, and mRNA was harvested for subsequent qPCR analysis. (C) IL-6 and NO production were determined from the culture supernatant 24 hours post LPS stimulation. (D) Differential gene expression analysis between the control, IL-4 24 hours stimulated, and IL-4 trained BMDMs at day 6 was presented as a heatmap. (E) Control and IL-4 24 hours stimulated BMDMs were stimulated with LPS or left untreated for 4 hours. LPS upregulated genes were filtered out, and the expression level was ranked normalized according to the Log₂FC value between the control-LPS group and IL-4-LPS group. Genes were further divided into three clusters: trained (Log₂FC ≥ 0.5), unaffected (0.5 ≥ Log₂FC ≥ -0.5), and tolerant (Log₂FC ≤ -0.5). (F) Gene ontogeny analysis of genes in the trained clusters. (G) IL-13 stimulated BMDMs were stimulated with LPS for 4 hours, and mRNA was harvested for subsequent qPCR analysis for the expression of IL-6 and IL-12. IL-6 and NO production were determined from the culture supernatant 24 hours post LPS stimulation. *P < 0.05, unpaired, two-tailed Student's t-test. Data are representative of 3 independent experiments with 3 to 4 samples per group (mean ± SD).

Figure 3

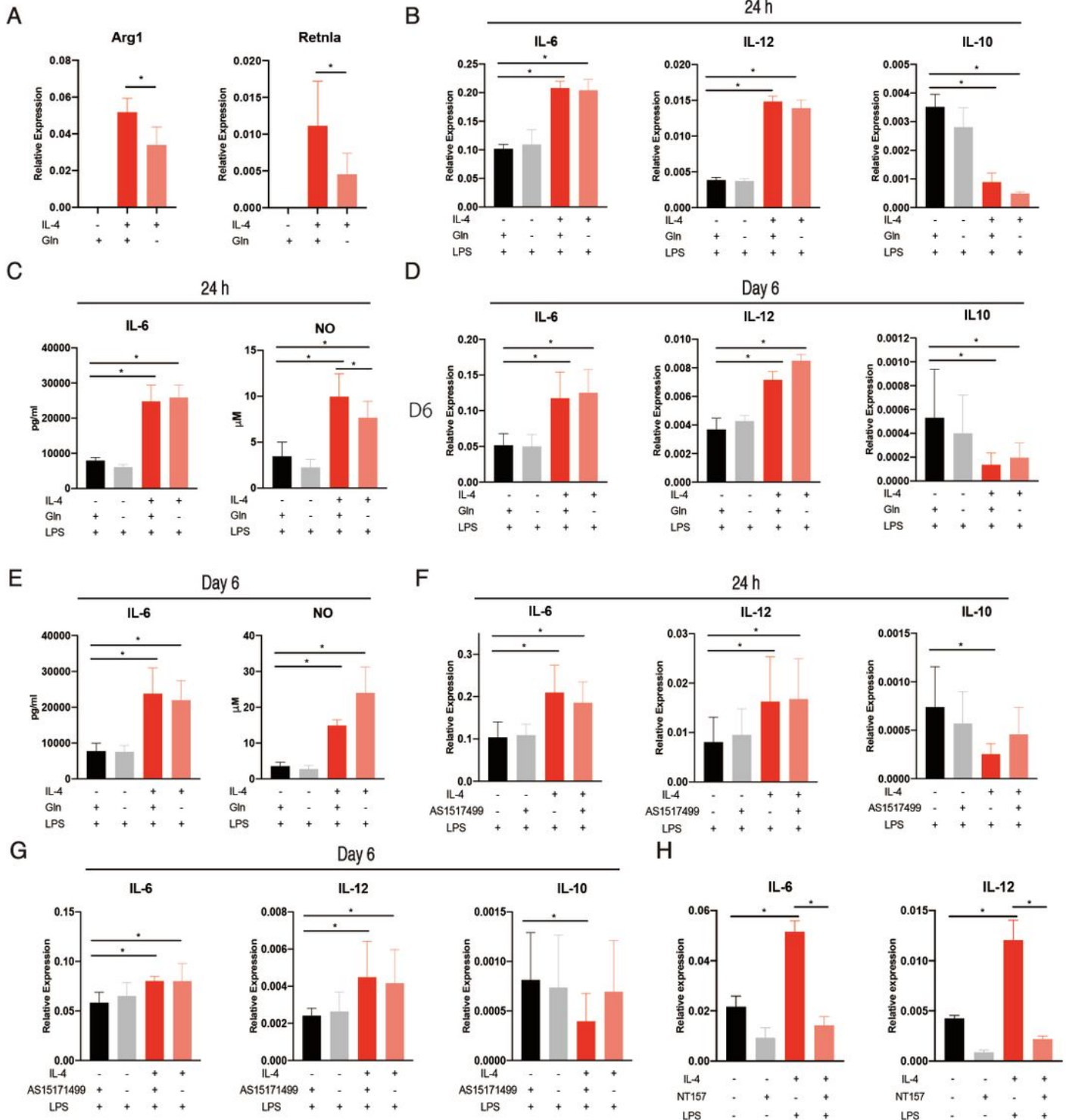


Figure 3

IL-4 induced trained immunity in a Gln/ α -KG/jmjd3 axis-, STAT6-independent and IRS-dependent manner. qPCR mRNA expression of M2 marker genes (A), cytokine genes (B, D, F, G&H) in BMDMs stimulated with IL-4 (A), or LPS (B, D, F, G&H) at 24 hours or day 6 post-IL-4 stimulation under various culture condition as indicated. Corresponding IL-6 and NO production were measured from supernatant harvested 24 hours

post LPS stimulation (**C&E**). *P < 0.05, unpaired, two-tailed Student's t-test. Data are representative of 3 independent experiments with 3 to 4 samples per group (mean ± SD).

Figure 4

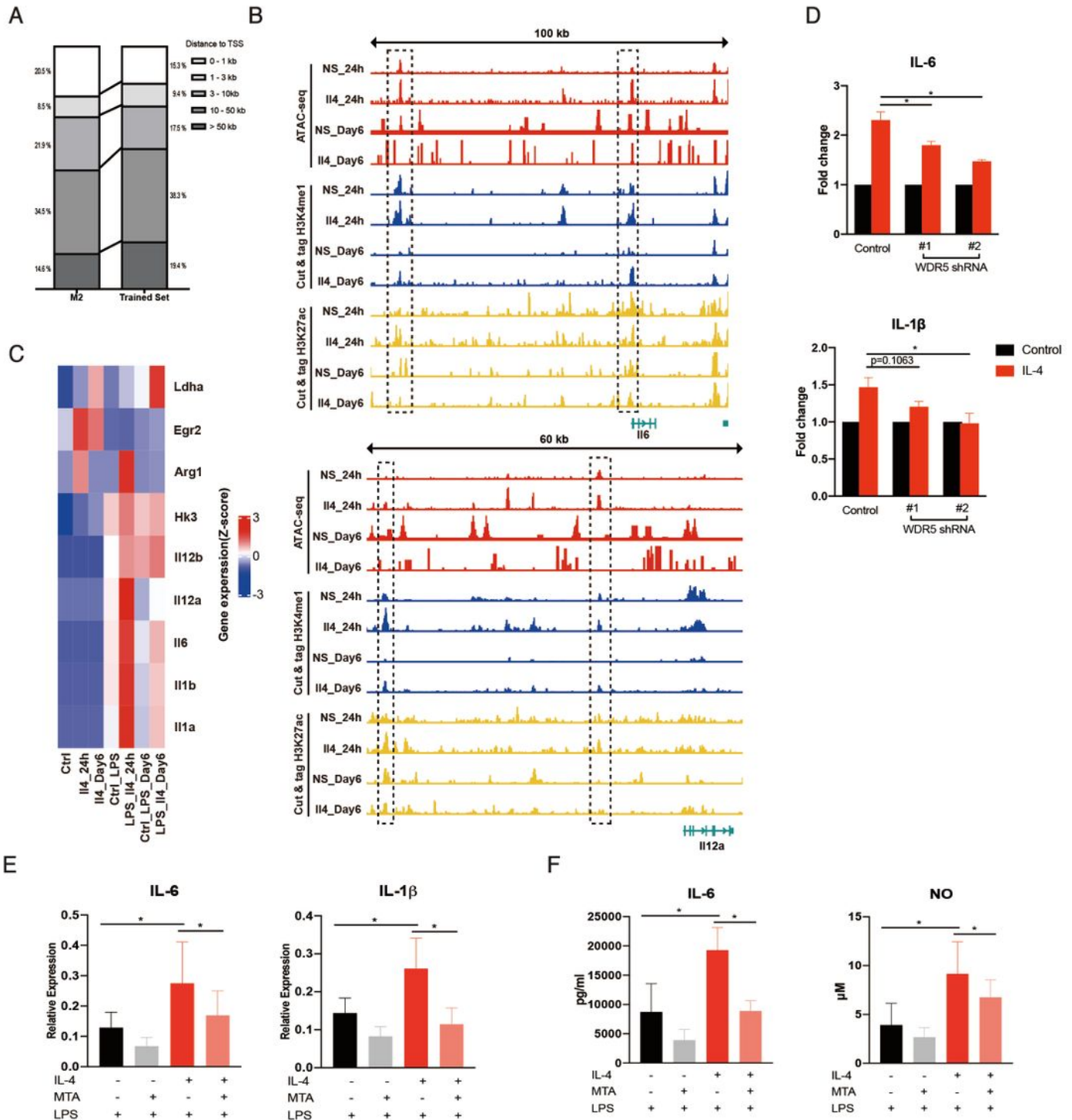


Figure 4

Epigenetic modification shapes IL-4 induced trained immunity in macrophages. (A) Peak distributions of differential ATAC peaks in M2 upregulated gene set and trained gene set between control and IL-4 treated

BMDMs. **(B)** Representative ATACseq H3K4me1, H3K4ac CUT & tag screenshots of control or IL-4 24h and day 6 stimulated BMDMs in the gene region pro-inflammatory genes IL-6 and IL-12a. The dashed box pointed to the poised enhancer region. **(C)** The gene expression profile of selected genes at basal state or 4h-post LPS stimulation. **(D)** Control or WDR5 stable knockdown Raw264.7 cells were pre-treated with IL-4 for 24 hours and stimulated with LPS for 4 hours to assess the mRNA expression of IL-6 and IL-1 β by qPCR. **(E)** qPCR mRNA expression of cytokine genes in BMDMs pre-treated with MTA for 30 minutes followed by 24 hours IL-4 stimulation. The gene expression was determined 4 hours post LPS stimulation. **(F)** IL-6 and NO production was determined from 24 hours supernatant post LPS stimulation. *P < 0.05, unpaired, two-tailed Student's t-test. Data are representative of 3 independent experiments with 3 samples per group (mean \pm SD).

Figure 5

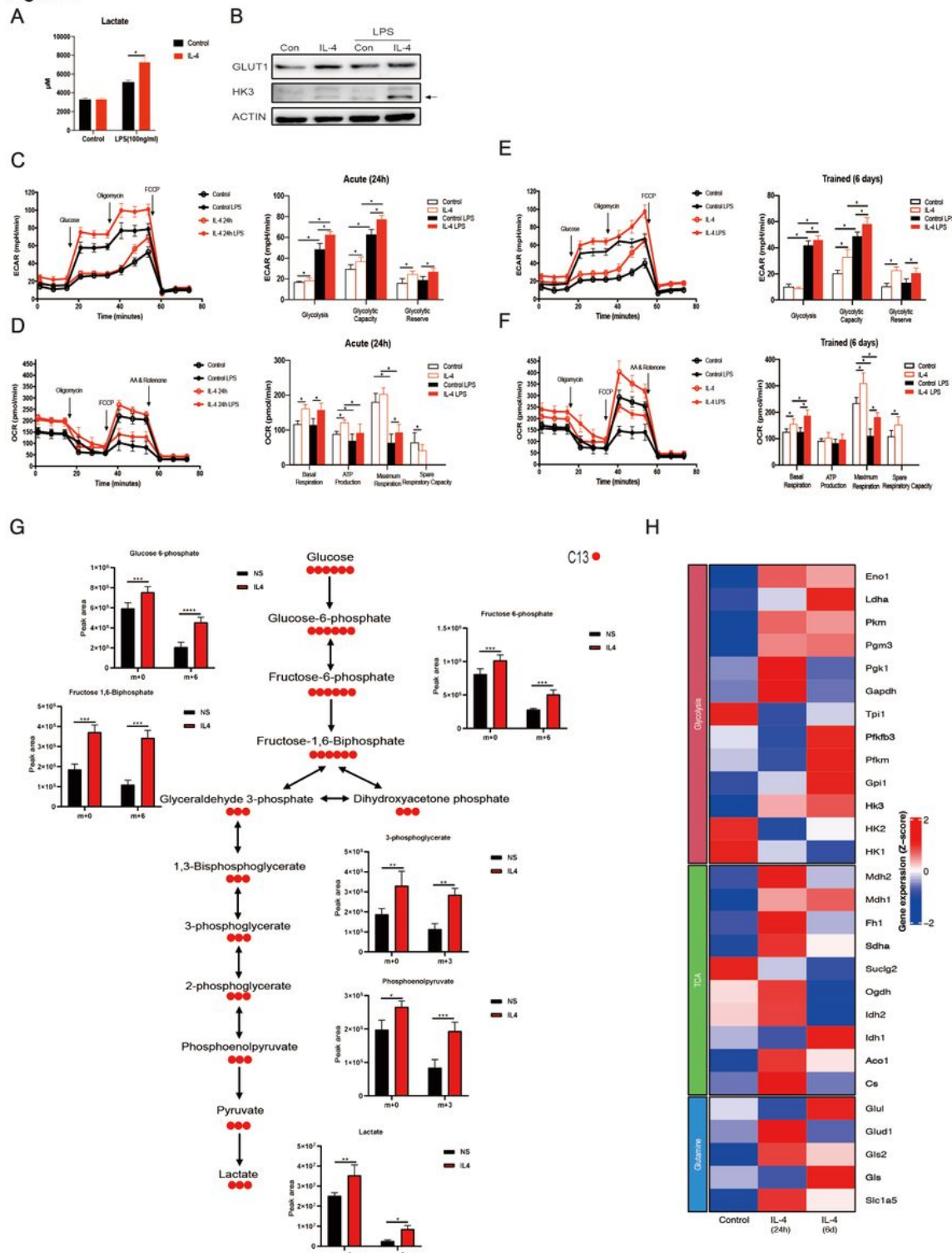


Figure 5

Metabolic characterization of IL-4 induced trained immunity in macrophages. (A) IL-4 trained BMDMs at day 6 were stimulated with LPS. The supernatant was harvested 24 hours post LPS, and lactate level was determined. (B) Western blot from cell lysate harvested from control or IL-4 trained BMDMs at day 6 or 3 hours post LPS stimulation. Antibodies specific for endogenous GLUT1, HK3 and actin were used to blot the target protein. Representative blots of three independent experiments are shown. Seahorse analysis

of control or IL-4 induced trained BMDMs at both acute (24h) or trained (6 days) at basal or 3 hours post LPS stimulation. ECAR and glycolysis capacity (**C&E**) and OCR and mitochondrial respiration capacity (**D&F**) were determined from two independent experiments. (**G**) Representative metabolites derived from $^{13}\text{C}_6$ -Glucose following the glycolysis pathway determined by LC-MS were shown. (**H**) Differential gene expression in glycolysis, TCA cycle, and glutamine metabolism between the control, IL-4 24 hours stimulated, and IL-4 trained BMDMs at day 6 was presented as a heatmap.

Figure 6

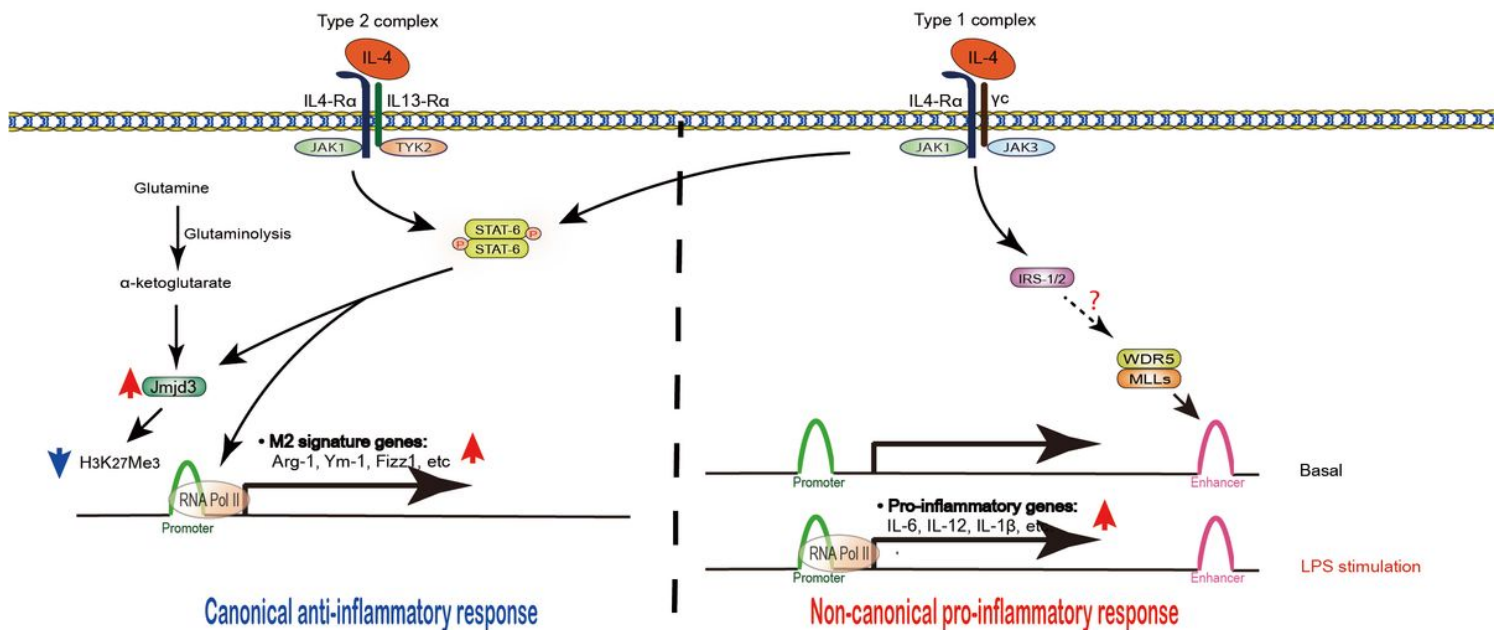


Figure 6

Schematic model of IL-4 induced canonical and non-canonical responses.

Supplementary Files

This is a list of supplementary files associated with this preprint. Click to download.

- [Supplementaryfigures.pdf](#)